Correlation of Flame Speed with Stretch in Turbulent Premixed Methane/Air Flames

JACQUELINE H. CHEN and HONG G. IM
Combustion Research Facility, Mail Stop 9051
Sandia National Laboratories
Livermore, California 94551-0969

Corresponding author:
Dr. Jacqueline H. Chen
Combustion Research Facility, MS 9051
Sandia National Laboratories
Livermore, CA 94551-0969, USA
Phone: (510) 294-2586
Fax: (510) 294-2595
email: jhchen@ca.sandia.gov

Word Count:
text: 3136 (estimate 392 words/page × 8.0 pages)
tables: 400 (2 × 200)
figures: 1800 (9 × 200)
total: 5336

Preferred Presentation:
Oral

Preferred colloquium topic area:
Turbulent flames (premixed)

Submitted to the 27th Symposium (International) on Combustion, Boulder, CO

DISCLAIMER

Abstract

Direct numerical simulations of two-dimensional unsteady premixed methane/air flames are performed to determine the correlation of flame speed with stretch over a wide range of curvatures and strain rates generated by intense two-dimensional turbulence. Lean and stoichiometric premixtures are considered with a detailed C_1-mechanism for methane oxidation. The computed correlation shows the existence of two distinct stable branches. It further shows that exceedingly large negative values of stretch can be obtained solely through curvature effects which give rise to an overall nonlinear correlation of the flame speed with stretch. Over a narrower stretch range, $-1 \leq Ka \leq 1$, which includes 90% of the sample, the correlation is approximately linear, and hence, the asymptotic theory for stretch is practically applicable. Overall, one–third of the sample has negative stretch. In this linear range, the Markstein number associated with the positive branch is determined and is consistent with values obtained from comparable steady counterflow computations. In addition to this conventional positive branch, a negative branch is identified. This negative branch occurs when a flame cusp, with a center of curvature in the burnt gases, is subjected to intense compressive strain, resulting in a negative displacement speed. Negative flame speeds are also encountered for extensive tangential strain rates exceeding a Karlovitz number of unity, a value consistent with steady counterflow computations.

Introduction

In the flamelet approach of turbulent premixed combustion, the flames are modeled as a wrinkled surface whose propagation speed, termed the "displacement speed," is prescribed in terms of the local flow field and flame geometry [1]. The response of the displacement speed, S_d, to flame stretch is then characterized by a Markstein number. Theoretical studies [2, 3, 4] suggest a linear relation between the flame speed and stretch for small values of stretch,

$$S_d/S_L^0 = 1 - MaKa, \tag{1}$$

where S_L^0 is the laminar flame speed, $Ka = \kappa\delta_F/S_L^0$ is the nondimensional stretch, or the Karlovitz number, and $Ma = \mathcal{L}/\delta_F$ is the Markstein number. The nominal flame thickness, δ_F, is determined as the ratio of the mass diffusivity of the unburnt mixture to the laminar flame speed. Flame stretch, κ, defined as the fractional rate-of-change of flame area, is expressed exactly as the sum of tangential strain rate, a_T, and a curvature term [5, 6, 7]

$$\kappa = a_T + S_d\nabla\cdot\mathbf{n} \tag{2}$$

where $\nabla\cdot\mathbf{n}$ is the flame curvature, and $\mathbf{n}$ is the flame normal vector.

In an actual implementation of a flamelet model in turbulent premixed flames, an accurate estimate of the Markstein number is crucial in predicting the turbulent flame speed, and thus the overall burning rate. Experimental measurement of flame speed and stretch in turbulent flames, however, is extremely difficult. As a consequence, measurement of flame speeds in strained flow fields is often made in simpler geometries [8, 9, 10], where the effects of transients associated with unsteady strain and large flame curvatures are often unaccounted for. Recent DNS with constant Lewis number along with experimental data obtained at the tip of a 2D Bunsen flame show the dependence of the displacement speed on stretch [11] due to negatively curved flames undergoing compressive strain. They show that the linear relation predicted by asymptotic methods applies to a much larger range of stretch values, and that strain and curvature effects can be parameterized by stretch alone. However, their data is limited to only negatively curved flames in steady state, and the computations do not account for differential diffusion of intermediate species which may be amplified at flame cusps.

In the present study results of direct numerical simulations of unsteady two-dimensional flames with detailed methane/air chemistry provide an alternative method of obtaining flame structure and propagation statistics. The primary objective is to determine the correlation between the displacement speed and flame stretch over a broad range of Karlovitz numbers, both positive and negative, and the distribution of stretch rates over the flame. The sensitivity of the location of evaluation of the displacement speed is determined using unburnt methane as a marker of the flame front. The observed response of the displacement speed is then interpreted in terms of local tangential strain rate and curvature effects.

Numerical Method

The numerical scheme is based on the solution of the Navier-Stokes, species and energy equations for a compressible gas mixture. The explicit finite difference algorithm uses a fourth-order low storage Runge-Kutta method for time advancement [12] and an eighth-order centered finite difference scheme for spatial differencing [13]. The chemical mechanism is based on a detailed C_1 mechanism for methane-air oxidation [14] with 17 species and 68 reversible reactions. The species mass diffusion is determined by prescribing the Lewis numbers of individual species [15], as presented in Table 1. The molecular viscosity of the mixture is temperature dependent, while the thermodynamic properties (enthalpy, specific heat) are temperature and composition dependent. The Prandtl number is taken to be 0.708.

The computations are initialized with a one-dimensional steady laminar flame profile. Fuel-lean to stoichiometric mixtures (equivalence ratio of 0.7 and 1.0) of methane/air are preheated to 800 K in the reactant freestream. The profiles are obtained from a one-dimensional steady code PREMIX [16], and the solution is allowed to adjust to the simplified transport in a one-dimensional DNS.

The turbulence is prescribed by an initial two-dimensional turbulent kinetic energy spectrum function [17] which is superimposed on the laminar flame

$$E(k) = A_k \frac{u'^5}{\epsilon} \frac{(k/k_e)^4}{\left[1+(k/k_e)^2\right]^{17/6}} \exp\left[-\frac{3}{2}\alpha_k \left(\frac{k}{k_d}\right)^{4/3}\right], \qquad (3)$$

where k is the wavenumber and ϵ is the turbulence kinetic energy dissipation rate; the constants A_k and α_k are equal to 1.5. In this equation, k_e is the wavenumber of the most

energetic scale and k_d is the wavenumber corresponding to the Kolmogorov dissipation scale. These parameters are evaluated using the integral constraints on the definitions of kinetic energy and dissipation rate in isotropic turbulence [17]. The ratio of the turbulence intensity to the laminar flame speed, u'/S_L^0, is taken to be ten, and the ratio of the integral eddy scale to the thermal thickness, L_{11}/δ, is 3.0. The turbulence Reynolds number based on L_{11} and the unburned gas properties at 800 K is 181. The computational domain size is 0.67 cm, or 21.6δ, in the directions parallel and perpendicular to the laminar flame. The thermal thickness, δ, is 4.48 times the nominal flame thickness, δ_F. The domain is resolved into 750 uniform grid points in each direction.

The Displacement Speed: Location of Evaluation and Definition

The direct numerical simulation results are used to evaluate the flame speed in terms of the displacement speed of an isoline representing the flame front. For finite-thickness flames described by multi-step chemical kinetics, the choice of location of S_d evaluation in the flame is somewhat ambiguous, because the theoretical formulation is based on asymptotically thin flames. Experiments in steady laminar flames [18, 19], however, indicate that the burning velocity is most likely to be reproducible and independent of variations in local geometry and flame curvature when measured in the thin primary reaction zone. Elsewhere in the flame, the measurements are subjected to cross–stream diffusion and lateral flow expansion effects by the flame.

Following the suggestion by Fristrom [18] and Dixon-Lewis and Islam [19], the isoline chosen in the present DNS corresponds to the 10 % value of the unburnt methane mass fraction which is within the primary reaction zone in the flame. This isoline is plotted for the lean case in Fig. 1 to indicate the degree of flame corrugation after 3.76 eddy turnover time. Here, the heat release isocontours are overlaid, confirming the adequacy of the particular choice of isoline for tracking the primary reaction zone. In Fig. 2, the sensitivity of the displacement speed to the choice of the isoline is examined by evaluating S_d along several representative flame normals. Most of the heat release is bracketed by methane mass fraction ranging between 5 to 30 % (denoted by the shaded region) of the unburnt value of 0.039. For

Fig. 1

Fig. 2

the range of curvatures and strain rates considered in the DNS, it is seen from Fig. 2 that the displacement speed remains nearly constant throughout the thin primary reaction zone, consistent with earlier experimental observations [18]. On the other hand, far upstream of the preheat zone, *e.g.* 90% of unburnt methane mass fraction, substantial changes in flame speed are observed.

The density-weighted displacement speed of the flame relative to the local gas velocity is defined as:

$$S_d^* \equiv \frac{\rho S_d}{\rho_o} = -\frac{\dot{\omega}_\alpha}{\rho_o \left|\nabla Y\right|} - \frac{\frac{\partial}{\partial \eta}\left(\rho D_\alpha \frac{\partial Y}{\partial \eta}\right)}{\rho_o \left|\nabla Y\right|} - \frac{\rho D_\alpha}{\rho_o}(\nabla \cdot \mathbf{n}) \tag{4}$$

where ρ_o denotes the density in the unburned state of the mixture, and η is the direction normal to the flame. The density-weighted formulation eliminates dilatational effects on the displacement speed, and has been shown, for low turbulence intensity, to yield a relatively constant value across the reaction zone [20]. Here, the subscript α is the index of the species for which the mass fraction isocontour is being tracked. The unit normal vector of the isoline is defined as

$$\mathbf{n} = -\frac{\nabla Y_\alpha}{\left|\nabla Y_\alpha\right|}. \tag{5}$$

and the flame curvature is defined as

$$C \equiv \nabla \cdot \mathbf{n}. \tag{6}$$

The three terms on the right hand side of (4), respectively, show that the value of the displacement speed is a result of the balance between reaction, normal diffusion and tangential diffusion, and is modulated by the value of the scalar gradient at the location where it is measured. It is noted that the tangential diffusion term is linearly proportional to the local curvature where the constant of proportionality is given by the local mass diffusion coefficient, D_α [21, 22]. The curvature is taken to be positive (negative) when the flame is convex (concave) to the unburnt gas.

Finally, the Markstein number and flame stretch given by Eqs. 1 and 2 are presented in terms of density–weighted values for S_d as

$$S_d^*/S_L^0 = 1 - MaKa, \tag{7}$$

where

$$Ka \equiv Ka_s + Ka_c = \delta_F/S_L^0(a_T + S_d^* \nabla \cdot \mathbf{n}). \tag{8}$$

Results and Discussion

We first examine the correlation of the displacement speed with the overall Karlovitz number, Ka, *i.e.* the sum of the tangential strain and curvature components. Since the lean and stoichiometric cases are found to be qualitatively similar, only the results for the lean case will be presented and discussed. However, the Markstein numbers for both cases are presented and compared against steady counterflow computations. For convenience, the superscript *, denoting the density–weighted description, is omitted in the discussion of the results.

The correlation of the displacement speed with Karlovitz number for the solution at 3.76 eddy turnover time is shown in Fig. 3. Three features are immediately evident: first, that there exists two distinct branches depending upon the sign of the displacement speed, second, that the correlation between flame speed and stretch is nonlinear, and third, that exceedingly large negative values of flame stretch exist for what appears to be a small percentage of the overall flame denoted by a relatively fewer number of data points in Fig. 3. The range of stretch rates experienced by the flame is between $-20 \leq Ka \leq 1.2$. Fig. 3

To substantiate the statistical significance of various portions of the data shown in Fig. 3, the probability density function (pdf) of the stretch rate is shown in Fig. 4. Although not shown here, from the pdf of the curvature we found that the range of flame curvatures is between $-1 \leq \nabla \cdot \mathbf{n}\delta_F \leq 3$, with a mean of zero. The overall shape of the pdfs are consistent with DNS results with simple chemistry [23]. Fig. 4

We also find in Fig. 4 that over 90 % of the flames are between $-1 \leq Ka \leq 1$, and the proportion of flames undergoing compression, or negative stretch, is 30%. This represents a significant fraction of the overall flame area and suggests a need to better understand how flames propagate in the presence of both compression and curvature. Incidentally, this result supports the recent study [24] based on statistical results of propagating surfaces from constant density DNS data, in which the model assumes that approximately one-third of the flames are undergoing compression.

Figure 5 further shows the pdf of the tangential strain rate only, *i.e.* Ka_s. By comparing Figs. 4 and 5, it is evident that the long negative tail shown in Fig. 4 is attributed solely to the curvature term, and not to tangential strain. Therefore, it appears that only a few

isolated regions of large negative stretch exist, even when the flame is subjected to high intensity turbulence. Fig. 5

Given the statistical importance of flame stretch within the range of $-1 \leq Ka \leq 1$, we first determine the displacement speed correlation of those points with stretch. The data in Fig. 3, replotted over a narrower range of stretch, is shown in Fig. 6. The upper branch shows that the displacement speed decreases with an increase in Ka (and therefore positive Ma from the definition in Eq. (1)), which is consistent with theoretical results for thermo-diffusively stable flames ($Le \geq 1$). The data further shows, within the limitation of the scatter in the data, that the dependency on stretch in this range is nearly linear. This demonstrates that the asymptotic theory, formally applicable to small values of stretch, can be applied over a broader range of strain rates and curvatures.

A least squares linear fit over the data in Fig. 6 yields a Markstein number which can be compared against fresh-to-burnt numerical counterflow data obtained using the same chemical mechanism. The comparison of Markstein numbers obtained from the DNS and the counterflow computations for both the lean and stoichiometric cases is summarized in Table 2. For the purpose of comparison the linear fits in both the DNS and the counterflow were made over the same range of stretch: $0 \leq Ka \leq 1$. The last column, a linear fit of the DNS data over a range extended to negative stretch, $-1 \leq Ka \leq 1$, gives a slightly larger value of the Markstein number, indicating a greater sensitivity of the burning velocity to compressive strain and curvature effects. Note that the relative error between the counterflow and DNS is less than 15% for both cases. The good agreement suggests that, over a wide range of stretch rates, curvature effects are interchangeable with strain rate effects in determining stretch effects on flame propagation. This conclusion implies that a significant part of the turbulent flame can be represented by plane strained flames. It is somewhat surprising that the agreement is so good, considering the unsteadiness associated with the turbulent flame. The scatter in the data is likely due to local unsteadiness in the flame, integrated over several eddy turnover times. Fig. 6

The negative branch in Fig. 6 may seem counter-intuitive, as it appears that for some portion of the flame the displacement speed increases with the Karlovitz number. However, by conditioning the correlation in Fig. 6 on local curvature (colored square symbols in Fig. 6),

it is found that this branch occurs in a region of large positive curvature, where the center of curvature is located in the burnt gases. In this case, the flame is convectively pulled upstream by strong turbulent eddies, such that the magnitude of the diffusive flux tangential to the flame front exceeds that of the adverse convective flux [21]. As a result, the flame retreats back towards the products and exhibits a negative displacement speed. Hence, the positive slope in the negative branch in Fig. 6 simply shows that the larger the positive curvature becomes, the faster the cusp retreats.

Negative flame speed can also be achieved purely by excessive tangential straining, where normal diffusion, as distinct from tangential diffusion at cusps, exceeds reaction locally, to counteract adverse convective fluxes [25, 26]. Note that negative flame speed does not imply negative consumption rates; rather, it implies that diffusion is the primary mechanism for bringing fresh reactants to the flame in the presence of adverse convective gradients. In the earlier stage of the DNS results when the turbulence intensity is the highest, negative displacement speed was observed for positive Karlovitz number in excess of unity as shown by the extension of the linear segment for $Ka > 1$ in Fig. 7. This is consistent with planar premixed counterflow computations in a fresh-to-burnt configuration shown in Fig. 8, where, at 10% unburnt methane, the crossover point to negative speeds occurs at $Ka = 0.722$, where $Ka \sim O(1)$. Note that isoconcentration lines of methane evaluated at the location corresponding to the half maximum of the heat release on the upstream side do not exhibit negative speeds; only isolines downstream of this location in the reaction zone cross over to the product gases. This is also consistent with the DNS results; the crossover to negative speeds occurs at a value of methane mass fraction equal to 20% of the unburnt value. In Fig. 7 we find that 20% of the flame is undergoing negative displacement speed due to extensive stretch. These regions experience incomplete combustion, or even partial extinction [25] as fuel consumption and heat release rates decrease to values as low as half of their maximum laminar values. Associated decreases in radical concentrations are also observed. We conjecture that the observed "bending" in the turbulent burning velocity at high turbulence intensity may be partly due to this phenomena, as a non-negligible fraction of the overall flame encounters incomplete combustion, lower consumption speeds, and ultimately lower turbulent burning velocity as the flames are pushed into the product gases. Further

Fig. 7

Fig. 8

simulations are required to explore this possiblity.

As a further remark regarding the curvature portion of stretch, we observe that large negative values of Karlovitz number are found to be due to the effect of strong curvatures; for these cases the correlation shows nonlinear behavior. The form of the nonlinearity can be determined by recasting Eq. (7) in terms of the Markstein number as

$$Ma = \frac{1 - S_d^*/S_l}{\delta_F/S_L^0(a_T + S_d^* \nabla \cdot \mathbf{n})} \tag{9}$$

and in the limit when $S_d^*/S_l \gg 1$ and $S_d^* \nabla \cdot \mathbf{n} \gg a_T$, we obtain

$$Ma \sim \frac{1}{\nabla \cdot \mathbf{n}}. \tag{10}$$

In Fig. 9 a scatter plot of S_d^* versus curvature clearly shows that the first criteria, $S_d^*/S_l \gg 1$, is satisfied in regions where the magnitude of curvature is large. The second criteria is also satisfied based on the earlier discussion on the distribution of stretch and tangential strain. The limiting behavior given by Eq. (10) is observed in Fig. 3, as the slope (Markstein number) tends towards zero for the points with large negative Karlovitz number. While the limiting behavior is the same, it is important to note the fundamental distinctions between positive and negative cusps, even if the Lewis number based on the global mixture is near unity as for the methane/air system considered in the present study [20]. The difference is partly due to diffusion of light radical species which focuses (defocuses) at negative (positive) cusps, and, thereby through chemical nonlinearity, affects global properties of the flame such as propagation speed, fuel consumption and heat release. This contrasts the conclusions drawn by Poinsot *et al.* [11] in which enhancement of the flame speed at the Bunsen flame tip was attributed to hydrodynamic and diffusive mechanisms, and not to chemical effects. In their study, the single-step global chemistry does not account for the preferential diffusion effects of intermediate species.

Fig. 9

For large negative curvatures (upper branch in Fig. 3), the displacement speed is enhanced, not only by differential diffusion and focusing of mobile radicals, but also by upstream flame-flame interaction. Local flame curvatures in excess of four thermal thicknesses are observed as a result of the intense turbulence. For a radius of curvature less than one thermal flame thickness, the flame starts to undergo mutual annihilation with neighboring

flames as their respective thermo-diffusive and reactive layers start to merge. This interaction leads to further acceleration of the flames due to vanishing species gradients and shifts in balance between chemical reaction and normal diffusion as the cusp retreats [27]. On the other hand, when the flame is positively curved, in the limit of large curvature, the displacement speed becomes linearly proportional to the local curvature, or diffusion tangential to the flame surface [21]. The contributions from normal diffusion and reaction in this configuration are minimal.

Concluding Remarks

Two-dimensional unsteady DNS data for lean and stoichiometric premixed methane-air flames has been used to determine the correlation of displacement speed with flame stretch. It was observed that for the high turbulence intensity encountered by the flame, the correlation exhibits two distinct stable branches. The overall correlation is found to be nonlinear, with the source of nonlinearity derived from the curvature term. The nonlinear dependence is found to be inversely proportional to the local flame curvature in the limit of large curvature. The large magnitudes of the displacement speed encountered at the cusps serve as a stabilizing mechanism to counter the effect of the intense turbulence, resulting in a reduction in the overall turbulent flame area. For intense compressive strain at positive cusps, a second stable branch in the correlation arises due to negative flame propagation brought on explicitly by the positive local curvature.

The contribution of the tangential strain rate is found to be linear and continuous going from positive to negative values. We find it remarkable that the linear relation (Eq. (1)) is an excellent approximation for stretch rates far larger ($Ka \sim O(1)$) than what it was formally derived for ($Ka \ll O(1)$). We conclude that, given the wide distribution of curvatures and unsteady strain rates encountered in the DNS, and the good agreement between the Markstein numbers obtained from the DNS and the counterflow computations, a single parameter, namely the overall Karlovitz number, can be used to correlate unsteady strain and curvature effects on turbulent flame propagation over a statistically relevant range of stretch, $-1 \leq Ka \leq 1$. Further work is needed, however, to properly address the issue of flow unsteadiness.

Acknowledgments

This research was supported by the United States Department of Energy, Office of Basic Energy Sciences, Chemical Sciences Division. The authors thank Dr. Tarek Echekki for many insightful discussions.

References

[1] Williams, F. A., "The Mathematics of Combustion" (J. D. Buckmaster, Ed.), *Society for Industrial and Applied Mathematics*, Philadelphia, 1985, pp. 97-131.

[2] Clavin, P. and Williams, F. *J. Fluid Mech.*, 116:251 (1982).

[3] Pelce, P. and Clavin, P., *J. Fluid Mech.*, 124:219 (1982).

[4] Matalon, M. and Matkowsky, B. J., *J. Fluid Mech.*, 124:239 (1982).

[5] Matalon, M., *Combust. Sci. Tech.*, 31:169 (1983).

[6] Pope, S. *Int. J. Engng Sci.*, 26:445 (1988).

[7] Candel, S. and Poinsot, T., *Combust. Sci. Tech.*, 70:1 (1990).

[8] Bradley, D. Gaskell, P. H. and Gu, X. J., *Combust. Flame*, 104:176 (1996).

[9] Taylor, S. C., Ph. D. Thesis, University of Leeds, Leeds, (1991).

[10] Tseng, L. K., Ismail, M. A., and Faeth, G. M., *Combust. Flame*, 95:410 (1993).

[11] Poinsot, T., Echekki, T. and Mungal G.,*Combust. Sci. and Tech.*, 81:45, (1992).

[12] Kennedy, C. A. and Carpenter, M. H., in preparation (1997).

[13] Kennedy, C. A. and Carpenter, M. H., *Appl. Num. Math.*, 14:3 (1996).

[14] Warnatz, J., Maas, U. and Dibble, R., *Combustion: Physical and Chemical Foundations, Modelling, Pollutant Formation*, Springer-Verlag, Heidelberg, Germany, (1996).

[15] Smooke, M. D. and Giovangigli, V., in *Reduced kinetic mechanisms and asymptotic approximation for methane-air flames* (Smooke, M. D. Ed.), Lecture Notes in Physics, no. 384, pp. 1-28, Springer-Verlag, New York, (1991).

[16] Kee, R. J., Grcar, J. F., Smooke, M. D. and Miller, J. A., Sandia National Laboratories Report SAND85-8240, (1985).

[17] Hinze, J. O., *Turbulence*, McGraw Hill, New York, 1975.

[18] Fristrom, R. M., *Physics of Fluids* 8:273 (1965).

[19] Dixon-Lewis, G. and Islam, S. M., *Nineteenth (Int.) Symposium on Combustion*, The Combustion Institute, 1983, pp. 283–291.

[20] Echekki, T. and Chen, J. H., *Combust. Flame*, 106:184 (1996).

[21] Gran, I. R., Echekki, T. and Chen, J. H., *Twenty-Sixth (Int.) Symposium on Combustion*, The Combustion Institute, 1996, pp. 323-329.

[22] Echekki, T. and Chen, J. H., *The Contribution of Curvature to the Propagation of Turbulent Premixed Methane-Air Flames*, in preparation, 1997.

[23] Trouve, A. and Poinsot, T., *J. Fluid Mech.* 244:405 (1993).

[24] Kostiuk, L. and Bray, K., *Combust. Sci. and Tech.*, 95:193 (1994).

[25] Libby, P. A. and Williams, F. A., *Combust. Flame*, 44:287 (1982).

[26] Sohrab, S. H. Ye, Z. Y. and Law, C. K., *Twentieth (Int.) Symposium on Combustion*, The Combustion Institute, 1984, pp. 1957-1965.

[27] Chen, J. H., Echekki, T., and Kollmann, W., *submitted to Combust. Flame*, 1997.

Figure Captions

1. Isocontours of heat release rate after 3.76 eddy turnover time in a lean premixed methane air flame, $\phi = 0.7$. The black line corresponds to 10% of unburnt CH_4 mass fraction. The coordinates are normalized by the flame thermal thickness, δ, where $\delta = 4.48\delta_F$.

2. Displacement speed along selected flame normals as a function of methane mass fraction. —— lines correspond to high a_T and low $\nabla \cdot \mathbf{n}$; ····· line corresponds to large negative $\nabla \cdot \mathbf{n}$; —·— line corresponds to large positive $\nabla \cdot \mathbf{n}$. The shaded band, between 5 to 30% of the unburnt mass fraction of methane, denotes the region in which most of the heat release occurs.

3. Correlation of displacement speed with Karlovitz number, based on nominal flame thickness, $\delta_F = D_u/S_l$, for a premixed methane/air flame, $\phi = 0.7$, at 3.76 eddy turnover time.

4. Probability density function of normalized stretch rate, Ka, evaluated at the flame surface, 10% unburnt CH_4, at 3.76 eddy turnover time.

5. Probability density function of normalized tangential strain rate, Ka_s, evaluated at the flame surface, 10% unburnt CH_4, at 3.76 eddy turnover time.

6. Correlation of displacement speed with stretch rate for a premixed meth ane/air flame, $\phi = 0.7$ at 3.76 eddy turnover time conditioned on curvature: pink ▫ $-1.0\delta \leq \nabla \cdot \mathbf{n} \leq 1.0\delta$, black ▫ $-1.2\delta_F \leq \nabla \cdot \mathbf{n} \leq 1.0\delta$, blue ▫ $1.0\delta \leq \nabla \cdot \mathbf{n} \leq 3.0\delta_F$.

7. Correlation of displacement speed with stretch rate for a premixed met h ane/air flame, $\phi = 0.7$ at 1.0 eddy turnover time. Note the linear segment showing negative flame speed for $Ka \geq 1$.

8. Correlation of displacement speed with normalized stretch rate, Ka, for 1D steady counterflow computation in a fresh-to-burnt configuration. for methane-air flame, $\phi = 0.7$.

9. Correlation of displacement speed with curvature for a premixed methane-air flame, $\phi = 0.7$, at 3.76 eddy turnover time.

species	Le
H_2	0.30
O_2	1.11
O	0.70
OH	0.73
H_2O	0.83
H	0.18
HO_2	1.10
H_2O_2	1.12
CH_4	0.97
CO	1.10
CO_2	1.39
CH_2O	1.28
CHO	1.27
CH_2OH	1.30
CH_3OH	1.30
CH_3	1.00
CH_3O	1.30

Table 1: Lewis numbers of species considered in the computations.

$\phi = 1.0$	$0 \leq Ka \leq 1$	$0 \leq Ka \leq 1$	$-1 \leq Ka \leq 1$
% unburnt Y_{CH_4}	**1D steady counterflow**	**2D unsteady DNS**	**2D unsteady DNS**
5	2.06	2.00	2.30
10	1.93	1.91	1.98
20	1.76	1.80	1.62
$\phi = 0.7$	$0 \leq Ka \leq 1$	$0 \leq Ka \leq 1$	$-1 \leq Ka \leq 1$
% unburnt Y_{CH_4}	**1D steady counterflow**	**2D unsteady DNS**	**2D unsteady DNS**
5	1.55	1.78	1.91
10	1.40	1.55	1.59
20	1.22	1.13	1.15

Table 2: Comparison of Markstein number, Ma, based on nominal flame thickness, δ_F, between 2D unsteady and 1D steady strained cases for premixed methane/air at 800K.

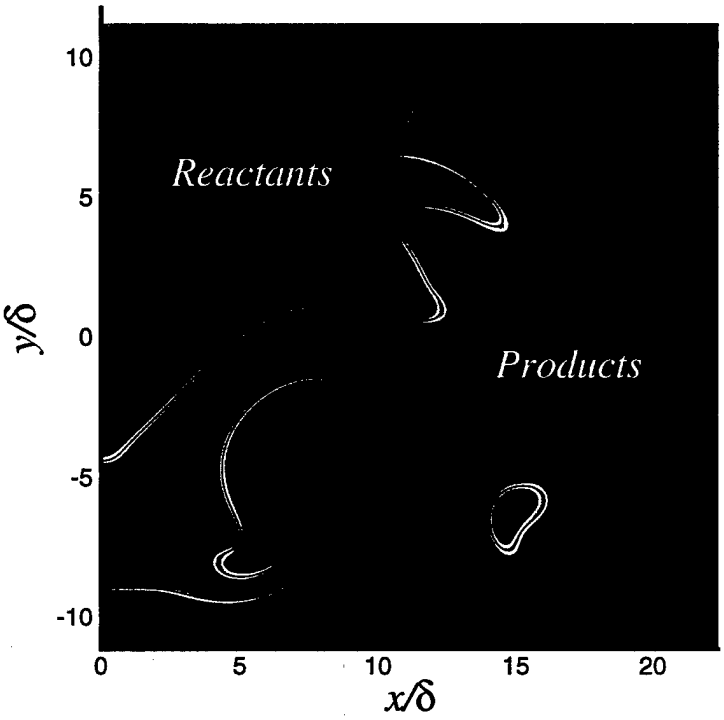

Figure 1: Isocontours of heat release rate after 3.76 eddy turnover time in a lean premixed methane air flame, $\phi = 0.7$. The flame speed is evaluated at the CH_4 mass fraction equal to 10% of its freestream value. The coordinates are normalized by the flame thermal thickness, δ, where $\delta = 4.48\delta_F$.

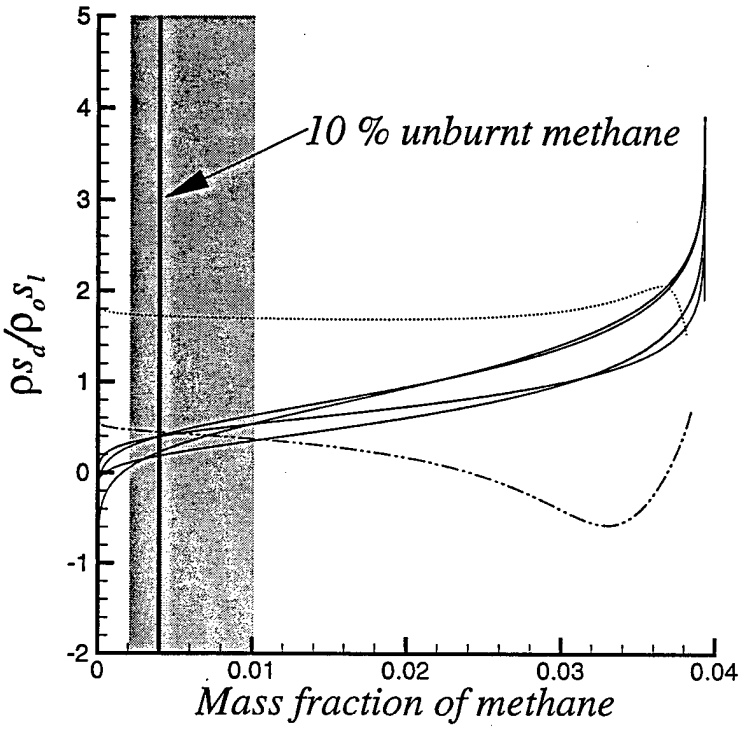

Figure 2: Displacement speed along selected flame normals as a function of methane mass fraction. —— lines correspond to high a_T and low $\nabla \cdot \mathbf{n}$; ····· line corresponds to large negative $\nabla \cdot \mathbf{n}$; —·— line corresponds to large positive $\nabla \cdot \mathbf{n}$. The shaded band, between 5 to 30% of the unburnt mass fraction of methane, denotes the region in which most of the heat release occurs.

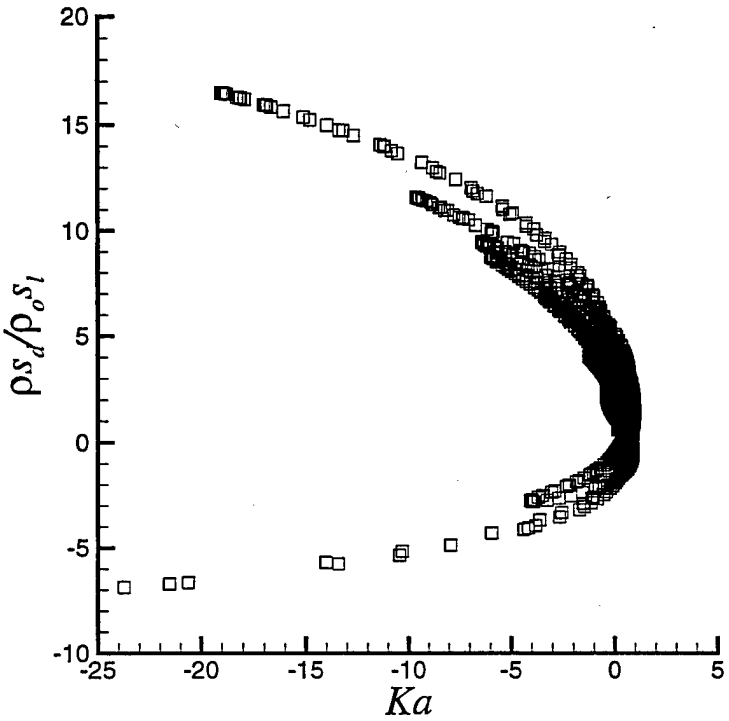

Figure 3: Correlation of displacement speed with Karlovitz number, based on nominal flame thickness, $\delta_F = D_u/S_l$, for a premixed methane/air flame, $\phi = 0.7$, at 3.76 eddy turnover time.

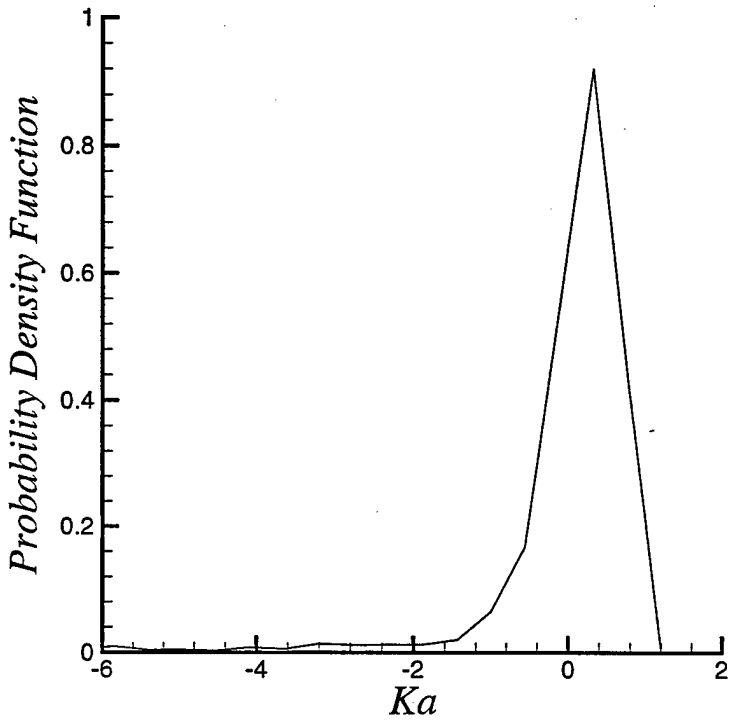

Figure 4: Probability density function of normalized stretch rate, Ka, evaluated at the flame surface, 10% unburnt CH_4, at 3.76 eddy turnover time.

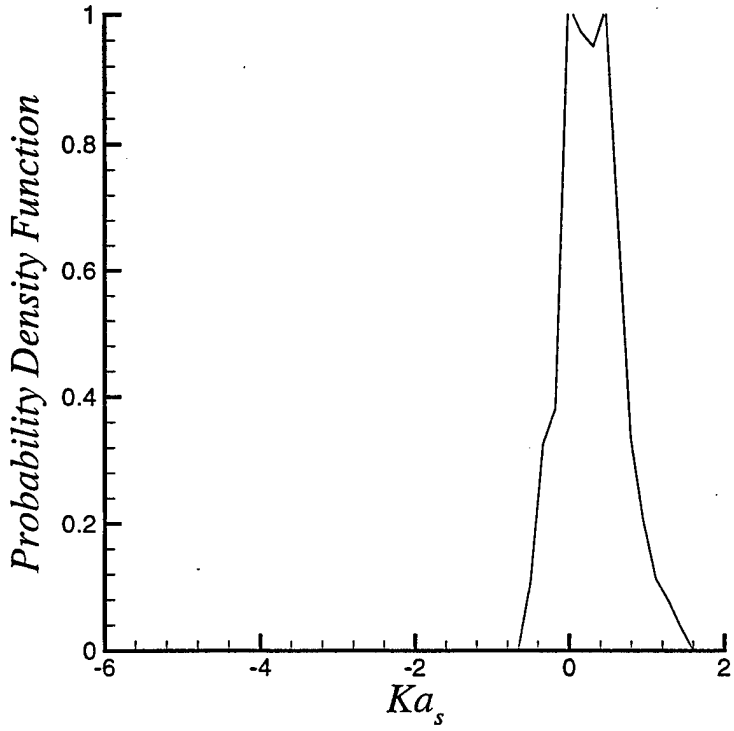

Figure 5: Probability density function of normalized tangential strain rate, Ka_s, evaluated at the flame surface, 10% unburnt CH_4, at 3.76 eddy turnover time.

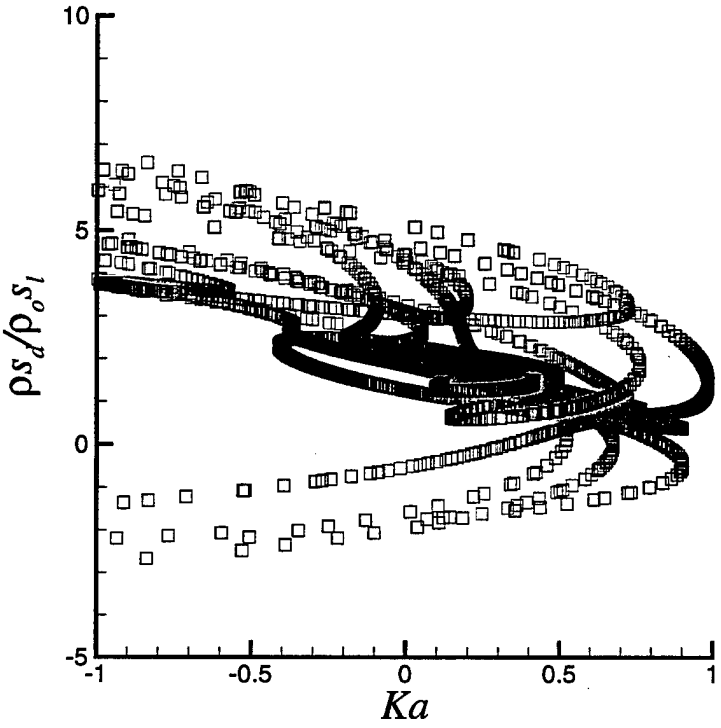

Figure 6: Correlation of displacement speed with stretch rate for a premixed meth ane/air flame, $\phi = 0.7$ conditioned on curvature: pink ▫ $-1.0 \leq \nabla \cdot \mathbf{n}\delta \leq 1.0$, black ▫ $-5.4 \leq \nabla \cdot \mathbf{n}\delta \leq 1.0$, blue ▫ $1.0 \leq \nabla \cdot \mathbf{n}\delta \leq 13.4$.

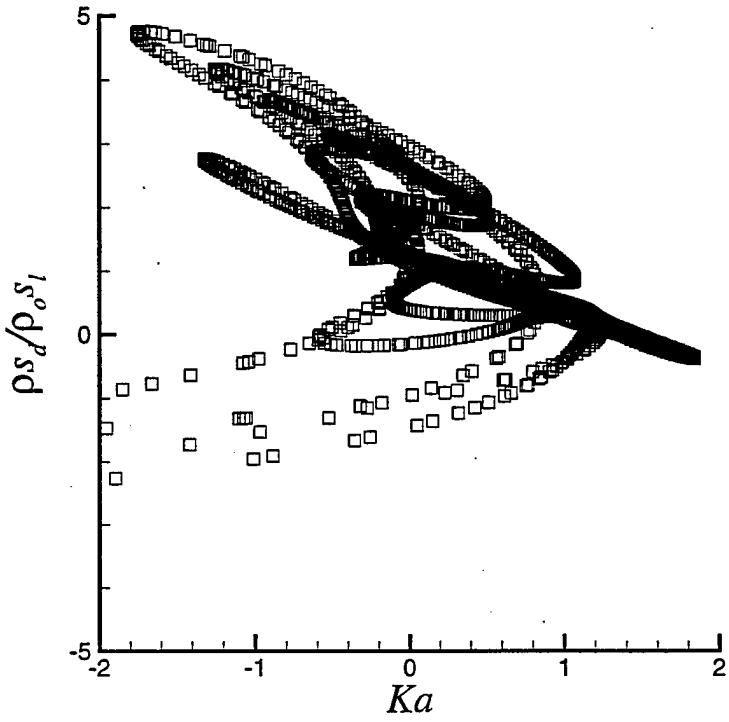

Figure 7: Correlation of displacement speed with stretch rate for a premixed meth ane/air flame, $\phi = 0.7$ at 1.0 eddy turnover time. Note the linear segment showing negative flame speed for $Ka \geq 1$.

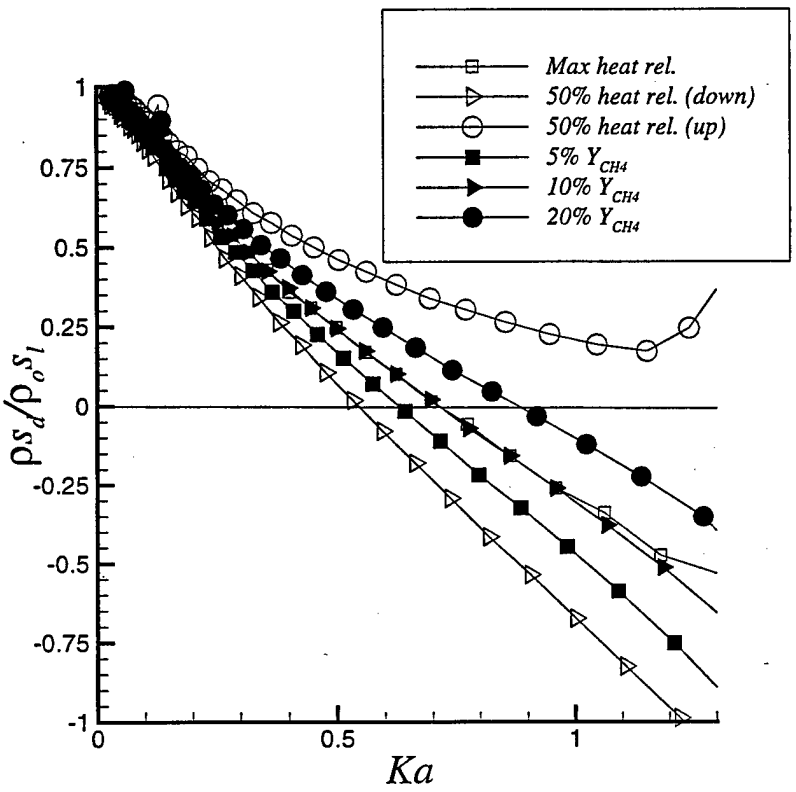

Figure 8: Correlation of displacement speed with normalized stretch rate, Ka, for 1D steady counterflow computation in a fresh-to-burnt configuration. for methane-air flame, $\phi = 0.7$.

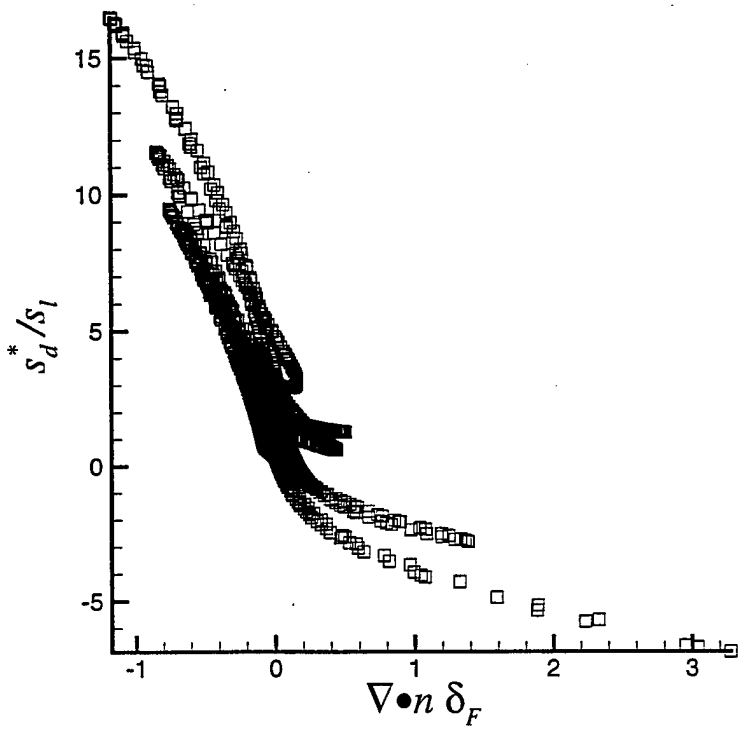

Figure 9: Correlation of displacement speed with curvature for a premixed methane-air flame, $\phi = 0.7$, at 3.76 eddy turnover time.

Report Number (14) SAND--98-8473C
CONF-980804---

Publ. Date (11) 199803
Sponsor Code (18) DOE/EE, XF
UC Category (19) UC-1409, DOE/ER